Photochronocoulometric Measurement of the Coverage of Surface-Bound Dyes on Titanium Dioxide Crystal Surfaces †

ARTICLE *in* THE JOURNAL OF PHYSICAL CHEMISTRY B · JANUARY 2007

Impact Factor: 3.3 · DOI: 10.1021/jp064529f · Source: PubMed

Photochronocoulometric Measurement of the Coverage of Surface-Bound Dyes on Titanium Dioxide Crystal Surfaces†

Yunfeng Lu,‡ Mark T. Spitler,§ and B. A. Parkinson*,‡

Department of Chemistry, Colorado State University, Fort Collins, Colorado 80523, and National Renewable Energy Laboratory, 1617 Cole Boulevard, Golden, Colorado 80401

Received: July 17, 2006; In Final Form: August 11, 2006

Atomically flat terraced single-crystal anatase and rutile surfaces can be prepared allowing for the reproducible adsorption of covalently attached sensitizing dyes. Once reproducible surfaces and dye coverages are achieved, a photochronocoulometric technique is developed to measure the surface coverage of the dyes, an important parameter in determining the efficiency of sensitization. The surface-bound dyes are irreversibly oxidized by exposure to a light pulse with the n-type oxide semiconductor electrode held in depletion. A double-exponential decay of the subsequent photocurrent is then measured, where the integration of the faster decay is associated with the adsorbed dye coverage and the second much slower decay is attributed to trace regenerators, including water, in the nonaqueous electrolyte. The ruthenium-based N3 dye shows the expected linear dependence of the rate constant on light intensity whereas a dicarboxylated thiacyanine dye shows a square root dependence of its photooxidation rate on light intensity. The sublinear response of the thiacyanine dye is discussed in terms of the more complex surface chemistry that is known for this family of sensitizing dyes.

Introduction

Chronocoulometry and double potential step chronocoulometry[1,2] were developed to measure the surface concentration of adsorbed electroactive species in the presence of additional diffusing electroactive species. The technique was used to measure the coverage of many adsorbed metal complexes on Hg electrodes.[1,3] Mercury electrodes were favored because they provide a reproducible and renewable electrode surface necessary for the discrimination of background charge (charging currents) from charge due to adsorbed electroactive species. The technique was extended to semiconductor surfaces where the adsorption of I_3^- as a function of concentration onto WSe_2 surfaces was measured using light, rather than a potential step, to initiate the photooxidation of adsorbed I_3^-. WSe_2 was a usable substrate due to its atomically flat surface and the ability to renew the surface via cleavage of the two-dimensional crystal resulting in reproducible surfaces and low capacitance backgrounds.[4]

We have been studying dye sensitization of oxide surfaces of low-index faces of the anatase and rutile forms of TiO_2 by covalently attaching dyes to the surfaces.[5−7] To enable these studies methods to reproducibly prepare these oxide surfaces with clean and atomically flat surfaces were developed.[8] The structure and the dynamics of the photoinjected electron-transfer processes of these dye-covered surfaces are important for understanding and improving the operation of dye-sensitized solar cells. Incident photon-to-current conversion efficiency (IPCE) values are measured as a function of dye concentration in the solution from which the covalent attachment is made. Adsorption isotherms for a particular dye/surface combination are then inferred using the assumption that the IPCE is proportional to the dye coverage.[5−7] Since the surface often contains multiple forms of the dye (monomers, dimers and higher aggregates), it is difficult to determine if these species have different efficiencies for photocurrent generation. High absorbed photon-to-current conversion efficiencies (APCEs) are the more important parameter for constructing efficient dye-sensitized solar cells. To determine APCE values the amount of adsorbed dye and the extinction coefficient of the adsorbed dye are required. (In nanocrystalline solar cells, the light-harvesting efficiency is nearly 100%, and so the absorbance value is not needed.) The surface coverage of the adsorbed dye molecules onto the TiO_2 nanocrystalline thin films can be determined by desorbing the dye and measuring the optical absorbance of the solution due to the large amount of adsorbed dye.[6] Gratzel et al. have measured the dye coverage on nanocrystalline anatase films by electrochemical oxidation of the dye and assumptions about the surface area of the nanocrystalline film.[9] Spitler and Calvin used the absorbance of the dye desorbed from multiple single-crystal surfaces; however, even using many expensive crystal plates resulted in a rather small absorbance in the solution.[10] Another method is to construct a single-crystal attenuated total reflectance (ATR) prism from the semiconductor of interest, where the absorbance of the adsorbed dye is multiplied by the number of internal reflections. The ATR approach is complicated by the optical absorption introduced by the dopants that are necessary for electrical conduction.[11] In the absence of a direct measurement of the absorbance of the dye on the surface, the surface coverage was inferred from the assumption that the plateau of the isotherm, determined with the previously mentioned assumption that IPCE is proportional to coverage, represented a complete monolayer. A geometric model of the dye packing on the surface is then used to calculate the dye coverage.[12] The absorbance of the monolayer was then calculated using the bulk extinction coefficients. This method is not always accurate due to the

† Part of the special issue "Arthur J. Nozik Festschrift".

* Author to whom correspondence should be addressed. E-mail: Bruce.Parkinson@colostate.edu.

‡ Colorado State University.

§ National Renewable Energy Laboratory.

10.1021/jp064529f CCC: $33.50
Published on Web 09/27/2006

possible preferential orientation of the dye on the surface and the anisotropy of light absorption by many polar dyes.[10]

A simple direct measurement of the dye coverage would be a great benefit for the development of dye-sensitized solar cells since it would allow accurate measurements of APCE values on dye monolayers. Herein we present a simple photoelectrochemical method for measuring the coverage of dyes covalently attached to low-index anatase and rutile surfaces. In our method, we expose a dye-covered single-crystal oxide semiconductor surface, held at a potential in the depletion region, to a light pulse that photoexcites the dye with subsequent electron injection into the conduction band of the semiconductor. In the absence of a reducing agent (regenerator) in solution, the total photoinjected charge should be equal to the number of adsorbed dye molecules. Unlike conventional chronocoulometry, there is no current due to diffusing molecules, and the capacitance change, associated with the light pulse that is not absorbed by the semiconductor, is negligible, and so no background double-layer charging currents are produced.

Experimental Section

The rutile (100) single crystal was purchased from Commercial Crystal Laboratories, Ltd. The anatase samples were natural anatase crystals that were mined in Hargvidda, Tyssedal, Norway. These bipyramidal crystals exhibited low-energy growth surfaces with large wedge-shaped (101) faces and (001) end caps. The (101) crystal faces were dark blue, and the entire crystal was used. The doping densities determined with Mott Schottky analysis were in the range of $(1-5) \times 10^{19}$ for the anatase and 5×10^{18} for rutile. Atomically flat terraced surfaces for all polytypes and faces were prepared as described earlier.[8] Atomic force microscopy (AFM) (Digital Instruments Nanoscope IIIA controller and a multimode SPM) was used to characterize the polished surfaces. Silicon tips from MikroMasch with a 40 N/m force constant and resonant frequency around 170 kHz were used.

The crystal was mounted to the electrode using epoxy (Dexter Epoxy Patch) with Ga/In eutectic applied to the back of the electrode for an ohmic contact. After the epoxy set, the electrode was sealed with silicone rubber (RTV) and allowed to dry for a few hours. Before photoelectrochemical experiments the crystal was polished with a soft polishing cloth using 20 nm colloidal silica (Buehler, Inc.) and cleaned with 0.2 M NaOH, followed by a Milli-Q (18 MΩ) water rinse. The electrodes were then cleaned by illuminating at 0.6 V vs Ag/AgCl in 1 M HCl (for anatase) or 10 mM $NaClO_4$ (for rutile) for 5 min using an Oriel 150 W Xe lamp followed by an ethanol (Pharmaco, ACS grade) rinse. To allow the UV illumination to reach the sample surface a quartz electrochemical cell was used.

Cis-di(thiocyanato)-bis(2,2′-bipyridyl-4,4′-dicarboxylate) ruthenium(II) (usually referred to as N3) and *cis*-di(chloro)-bis-(2,2′-bipyridyl-4,4′-dicarboxylate) ruthenium(II) were obtained from Professor C. Michael Elliott. A 0.22 mM N3 dye solution and a 0.18 mM G7 dye solution (both dissolved in ethanol) were used to adsorb the dyes onto the cleaned crystal surfaces. These concentrations correspond to the plateau regions of the respective isotherms and so represent the maximum obtainable dye coverage.[5,7] Chart 4 software (ADInstruments) was used to record the photocurrent signal from a RDE4 potentiostat (Pine Instrument Company) using a 532 nm diode laser as the light source with the beam expanded to illuminate the entire crystal surface. The cell was degassed with N_2 gas before all measurements. The surface areas of the rutile (100) and anatase (101) electrodes were 0.20 and 0.32 cm^2, respectively.

The transient photocurrent measurements were made in a three-electrode configuration with a platinum counter electrode and a Ag/AgCl reference electrode. Acetonitrile (Fisher, optima grade) electrolyte was used containing 10 mM tetrabutylammonium perchlorate (Fluka, electrochemical grade) as a supporting electrolyte. Blank photoamperometric experiments with no dye present produced no photocurrent on the current scales used for measuring the photocurrent transient with adsorbed dye. Blocking the light during a photocurrent transient measurement with adsorbed dye resulted in the photocurrent immediately returning to the dark baseline value with no cathodic transient.

Results and Discussion

A photoexcited dye adsorbed onto the surface of an n-type semiconductor under depletion will inject the photoexcited electron into the conduction band of the semiconductor resulting in a photocurrent. This process is described by the following equations:

$$\mathrm{M} \xrightarrow{h\nu} \mathrm{M}^* \tag{1}$$

$$\mathrm{M}^* \xrightarrow{\text{fast}} \mathrm{M}^+ + \mathrm{e}^-_{(\text{semiconductor})} \tag{2}$$

Many measurements of the time scale of dye-sensitized electron injection into semiconducting nanocrystalline TiO_2 show that this process occurs on a subpicosecond time scale.[13−16] We expect that the injection should be fast on a single-crystal TiO_2 surface as well. Therefore any measured transient photocurrent will be limited by the excitation rate of the adsorbed dye that is determined by the light intensity. If this photoexcitation process is a first-order reaction dependent upon time *t*, then the following equations can be derived upon integration and differentiation

$$[\mathrm{M}] = [\mathrm{M}]_0 \, \mathrm{e}^{-\epsilon L_p \Phi \mathrm{t}} \tag{3}$$

$$I(t) = -\frac{\mathrm{d}[\mathrm{M}]}{\mathrm{d}t} AF = \epsilon L_\mathrm{p} \Phi AF [\mathrm{M}]_0 \, \mathrm{e}^{-\epsilon L_\mathrm{p} \Phi t} \tag{4}$$

where ϵ is the absorption cross section of the dye in $cm^2\ mol^{-1}$, L_p is the photon flux in mol $cm^{-2}\ s^{-1}$, Φ is the photochemical yield for electron transfer, A is the surface area of the TiO_2 electrode in cm^2, F is the Faraday constant, and $[M]_0$ is the original surface concentration of the dye molecules in mol cm^{-2}. Equation 3 is derived with the knowledge that a monolayer of a chromophore on a surface absorbs about 1% of the incident light.[10] This allows a linear approximation to be made for the absorbance of the adsorbed dye and a derivation of the first-order expression of eq 3 for use on the millisecond time scale of these experiments.

N3 is a ruthenium-based dye that has been extensively studied as a sensitizer for nanocrystalline solar cells. We have previously studied the adsorption of N3 onto low-index anatase and rutile crystal surfaces;[5,6] however, we had no direct measurement of the surface coverage of the N3 dye. Therefore, we decided to first apply photochronocoulometry to determine the coverage of adsorbed N3 on single-crystal oxide surfaces. The structure, absorption, and action spectrum (adsorbed onto single-crystal rutile (100) surface) for N3 are shown in Figure 1. The photocurrent action spectrum showed a 10 nm red shift relative to its solution absorption spectrum. The electrochemistry of N3 in nonaqueous solutions has been studied by Bond et al.[17] At slow scan rates irreversible oxidations were observed at 0.45 and 0.83 V versus the ferrocene/ferricenium couple in acetonitrile. The first oxidation was assigned to solution-phase N3

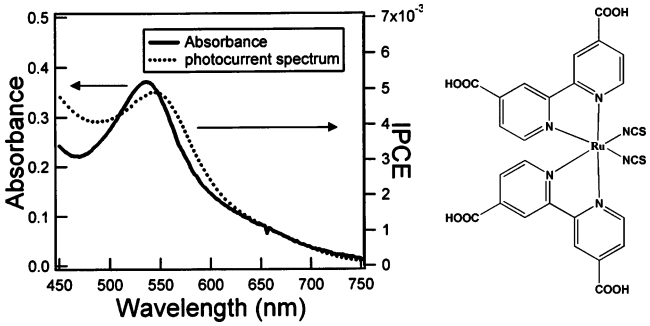

Figure 1. Molecular structure (right), solution absorption spectrum (solid line), and photoaction spectrum for the N3 dye adsorbed on a rutile (100) surface (dotted line).

while the second oxidation was assigned to the surface-bound dye. Wang et al. studied the oxidation of N3 surface-bound on mesoscopic TiO_2 and Al_2O_3 and found one oxidation at 0.38 V versus ferrocene/ferricenium.[9] Therefore, in the absence of N3 in solution, we can expect an irreversible one-electron oxidation of surface-bound N3.

A typical photochronoamperometric experiment was performed as follows: After the TiO_2 crystal electrode was UV cleaned, dye adsorption was accomplished by immersing the electrode into the dye solution. The electrode was rinsed and then immediately transferred to the electrochemical cell and allowed to equilibrate in the dark under potential control at 0.6 V for 30 s. With the semiconductor in depletion in the dark, there is almost no current flow across the blocking junction. The electrode was then exposed to 532 nm light from a diode laser, which is very near the maximum sensitization wavelength. Immediately after illumination a transient photocurrent is measured due to electron injection from the adsorbed dye into the conduction band of the TiO_2. The measured photocurrent transients for N3 adsorbed onto rutile (100) and anatase (101) are shown in Figures 2a and 2b. The photocurrent transient can be fit by a double-exponential decay that persists for much longer times. (This residual current will be discussed later.) A typical fit to the double-exponential decay is shown in Figure 2c. For the rutile (100) surface, the rate constant derived from the faster exponential decay shows a linear dependence with the light intensity, as shown in Figure 3a, as is expected from eq 3. At higher laser intensities (>12 mW), the measured rate constant begins to be sublinear probably due to the very fast photocurrent transient and the limited frequency response and data collection rate of the electronics used. The same dependence was measured for anatase (101) as shown in Figure 3b. The rate constant for photooxidaton of N3 on anatase (101) at a given laser power is a bit smaller than on rutile (100) perhaps due to variation in the laser power density on the two crystals.

The integrated current transient, or total charge from the fast decay (photochronocoulometric response), remains constant (2.0 $\pm$ 0.04 μC) at all laser powers as would be expected if the initial current is associated with the oxidation of a monolayer of adsorbed dye. Therefore, we use the integration of the fast current decay to determine the surface coverage of the adsorbed photoactive dye.

The transient photocurrent was also measured at different applied biases on the rutile (100) surface but at a constant light intensity (13.4 mW). As long as the applied bias is above a threshold value, just positive of the flat band potential of the TiO_2 single crystal, the derived rate constant and the collected charge remained constant at 2.2 $\pm$ 0.2 s^{-1} and 11 $\pm$ 1.0 $\mu C/cm^2$, respectively.

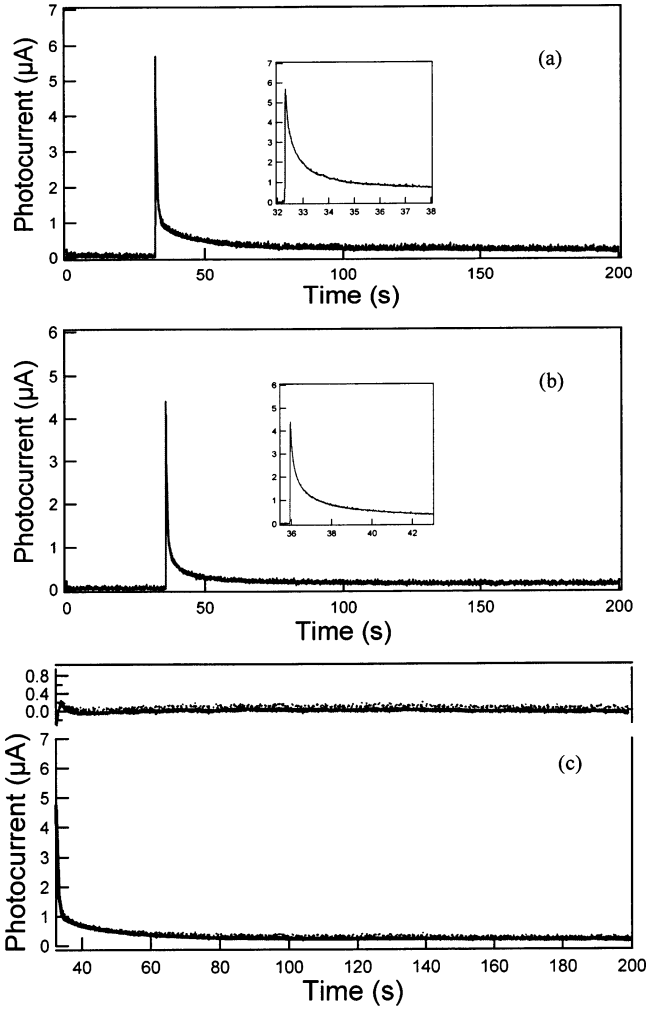

Figure 2. Transient currents for the photooxidation of N3 dye adsorbed onto (a) a rutile (100) surface and (b) an anatase (101) surface. The insets are enlargements at early illumination times. Part c shows the typical transient photocurrent (dots) and the fit to two exponential decays (solid line) and the residuals (top).

The surface coverage calculated from the integrated charge of the fast decay component is 1.0×10^{-10} mol cm^{-2} or 0.60 molecules nm^{-2} for the rutile (100) surface. The anatase (101) surface behaves similarly to the rutile (100) surface, as shown in Figure 3b, where the surface coverage was calculated to be 8.1×10^{-11} mol cm^{-2} or 0.5 molecules nm^{-2}. These numbers closely match the monolayer surface coverage of a close-packed N3 dye with the single-crystal TiO_2 surface[18] based on an area per N3 molecule of 1.8 nm^2.

The second slow current decay transient is problematic. In some cases the charge associated with the slow decay is up to 8 times the charge in the fast component. Blank experiments with no adsorbed dye produced no detectable sub-bandgap photocurrents on either anatase or rutile samples at the current scales used for the experiments with dye present. It is possible that SCN^- ions are released from oxidized N3 and act as regenerators of other adsorbed N3 molecules. However, the additional charge from this process would only double that measured in the fast current decay. Nonetheless, we tested whether this process contributes to the charge in the second decay by measuring the photocurrent transient for the identical complex except with Cl^- ligands replacing the SCN^- in N3. If chloride ion is released, its oxidation potential is too positive to act as a regenerator for oxidized N3. The total integrated

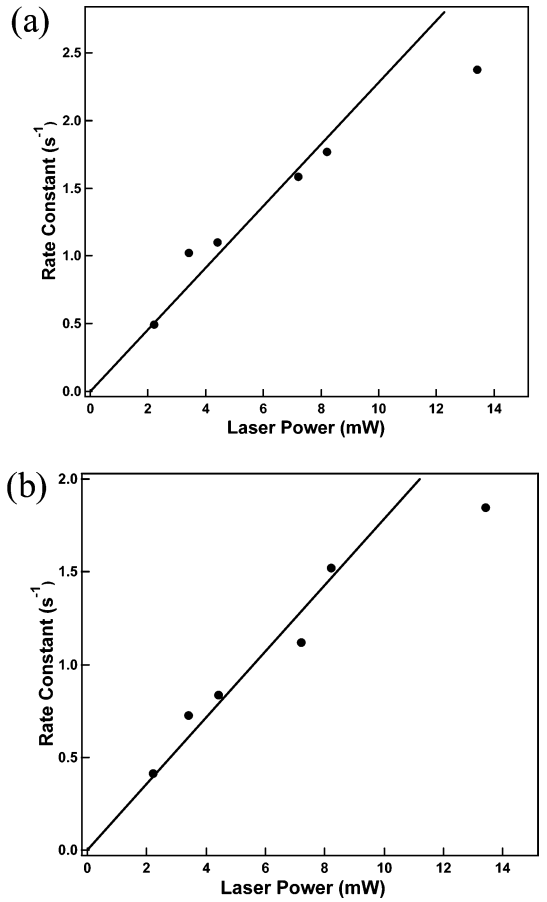

Figure 3. (a) Photooxidation rate constant for the N3 dye determined at different laser intensities for (a) rutile (100) surface and (b) anatase (101) surface. Solid lines are least-squares fits.

charges associated with the slow decay components were the same within experimental error for both ruthenium complexes. Another possibility for the slow decay would be the presence of small amounts of a reducing agent (regenerator) in the solution. Traces of hydroquinone, a regenerator used in previous sensitization experiments, adsorbed to the walls and frits of the electrochemical cell could contribute to this long decay. Therefore, we cleaned the electrochemical cell in piranha solution prior to repeating the experiment. This resulted in a reduction of the charge in the second component by about 70%, presumably due to traces of hydroquinone still leaching from the walls and glass frits of the cell from previous sensitization measurements where hydroquinone was present in high concentrations (4−5 mM) as a regenerator. However, even after consideration of both these mechanisms, there is still an unaccounted for charge that is up to 2.6 times larger than the charge in the fast component. The oxidized N3 dye adsorbed on nanocrystalline TiO_2 was reported to be stable for 75 min,[19] and so any trace of reducing agent would be able to regenerate dye for at least this long. We attribute the persistent residual sensitization current to a regeneration by the small amount of water always present in acetonitrile that has been exposed to the atmosphere. The oxidized N3 molecules or ruthenium-containing decomposition products have sufficient oxidation potential to oxidize water, and even if there were only a few water oxidation sites, the lateral charge transport observed for monolayers of N3 and related molecules on nanocrystalline TiO_2[6,9] would still allow for a small persistent regeneration of the photoactive dye.

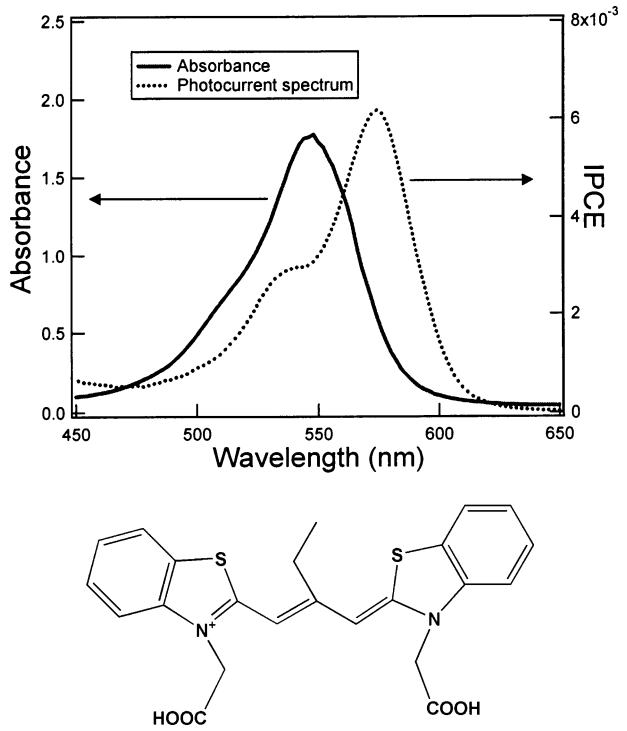

Figure 4. Molecular structure, solution absorption (solid line), and action spectrum (dashed line) of the G7 dye on a rutile (100) surface.

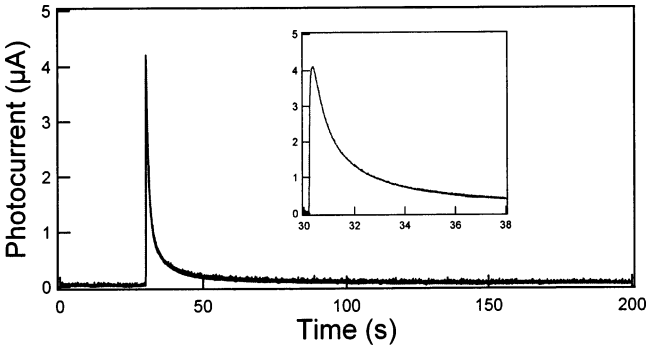

Figure 5. Transient photocurrent for photooxidation of G7 dye adsorbed on a rutile (100) surface. The inset shows an enlargement of the early time and shows the presence of a rise time.

We also studied the photochronocoulometry of the single-crystal rutile (100) surface with a dicaboxylated thiacyanine dye that we call G7. The structure, absorption, and photocurrent action spectrum of G7 are shown in Figure 4. The sensitization of anatase (101) single-crystal surfaces by this dye has already been reported.[7] The absorption spectrum peaks at 548 nm where only the monomer peak is present, whereas the photocurrent action spectrum is red-shifted by about 26 nm and also shows a blue-shifted sensitization peak associated with dimers. The structure of G7, with the ethyl group on the polyene bridge, prevents aggregation beyond the dimer.

Figure 5 shows the transient photocurrent generated from 532 nm laser illumination of G7 adsorbed onto a rutile (100) surface at an applied bias of 0.6 V. The photocurrent transient is similar to that measured for N3 and can also be fit with a double-exponential decay; however, there are some distinct differences that will be discussed below. The monolayer coverage derived by integrating the fast decay component was 4.1×10^{-10} mol cm^{-2}. The integrated charge from the slow component was about twice that of the fast decay component (75−90 μC/cm^2). If further oxidation occurs, then this accounts for about half of

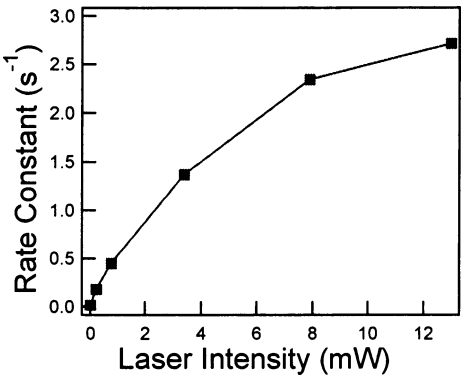

Figure 6. Photooxidation rate constant for the G7 dye adsorbed on a rutile (100) electrode measured at different laser intensities.

the charge from the slow decay component. The other half of the charge should be due to trace regenerator present in the solution, as was the case with the N3 study experiments discussed above. However, the residual currents in the case of G7 are less than half those measured for N3 since water oxidation should not be contributing in this case due to the absence of catalysis by ruthenium.

The dependence of the rate transient photocurrent decay for photooxidation of G7 with laser intensity is shown in Figure 6. Interestingly the rate constant is proportional to the square root of the laser power rather than the expected linear dependence. The mechanistic explanation for the square root dependence on laser power is still unclear and needs further study. However, despite the lower than expected rate constant, the charge associated with the fast decay component remained constant at $40 \pm 3.0\ \mu C/cm^2$ at all laser intensities.

According to eq 3, the time constant for the decay of the photocurrent should be proportional to the term $\epsilon L_p \Phi [M]_0$. For comparable initial surface coverages ($[M]_0$), the decay of G7 should be faster than N3 since the ϵ for G7 is 5 times larger than that of N3 at the illumination wavelength (532 nm). Indeed, this faster decay is observed, as is evident in Figure 6 for the low-intensity photolysis experiments. The surface area per molecule derived from the coulometry is 2.4 molecules nm^{-2} that is, like N3, nearly a close-packed monolayer for this dye.

However, G7 has a much more complicated photochemistry than N3. Parton and Lenhard have reported that the oxidized dye radicals for these types of cyanine dyes can dimerize in solution after electrooxidation.[20] Thus, the surface complement of oxidized G7 on TiO_2 should also be expected to dimerize. In addition, the electrochemical and absorption data for the dimer reveal that the dimer itself could sensitize photocurrent to the extent allowed by its internal photophysics.[20] The complexity of the G7 photochemistry is evident in the biphasic nature of the photochronocoulometric curve of Figure 6. The decline in photocurrent is preceded by a short 50−150 ms rise to the maximum, a feature that is not present in the N3 decay curves of Figure 5 where the maximum photocurrent is reached within the first several sampling intervals (10−20 ms). An analysis of the photocurrent decay in photochronoamperometry experiments must therefore consider these following reactions

$$2M^+ \rightarrow DH_2 \quad (5)$$

$$DH_2 \rightarrow D + 2H^+ \quad (6)$$

$$D + h\nu \rightarrow D^* \quad (7)$$

$$D^* \rightarrow D^+ + e^- \quad (8)$$

In reaction 5, the oxidized monomer dye dimerizes to produce the protonated dimer DH_2, which then subsequently releases two protons in reaction 6 to yield the dimer form D. Excitation of the dimer D may yield more photocurrent through reaction 8 and produce a singly oxidized dimer.

In the situation where D sensitizes photocurrent through reaction 8, a steady-state approximation for M^+ in reactions 2 and 5 allows one to derive the following expression for the photocurrent

$$j = AF\epsilon(M)L_p\Phi[M]_0 e^{-\epsilon(M)L_p\Phi t} + \left(\frac{1}{2}\right)\left[\frac{\epsilon(M)}{\epsilon(D) - \epsilon(M)}\right] AF(\epsilon(D)L_p\Phi[M]_0) \times \{e^{-\epsilon(M)L_p\Phi t} - e^{-\epsilon(D)L_p\Phi t}\} \quad (9)$$

where Φ is the quantum yield for electron transfer for the excited sensitizers, assumed to be equal for M and D.

The first term in eq 9 is the same as eq 3 and represents the decay of the monomer form of the dye. The second term represents the contribution to the current from the dimer form of the dye that can act as a sensitizer. It can be seen right away that the intensity dependence of the photocurrent of eq 9 will differ from that found for N3 in eq 3. However, the intensity dependence of the decay constant in eq 9 does not predict the observed behavior shown in Figure 6 where at higher light intensities the slope of the photocurrent becomes sublinear. This behavior would be consistent with the action of a quenching agent produced through the photochemistry of eqs 5−8, a species that is produced in higher concentrations at higher light intensities. This species may be an energy-transfer or electron-transfer quencher, but the former is implied by the observation that the integrated charge passed in the first fast decay is independent of light intensity: The preexponential factors of the terms in eq 9 are sublinear functions of light intensity.

A plausible species would be D^+, the radical dication form of the dimer since the dark oxidation of D is a two-electron process and the sensitization reaction 8 uses only one of the available electrons. It may also be that reaction 8 is negligible and the dimer itself then can serve as the quencher. With the available data, a definitive conclusion cannot be made for G7. A complete and thorough analysis of the complex photochemistry will require study of the dimer as a sensitizer as well as dyes that are variations upon the structure of G7 that do not dimerize. These studies are currently underway.

Conclusion

Surface coverages of both the N3 dye and the thiacyanine dye G7 adsorbed onto atomically flat single-crystal TiO_2 substrates were directly measured with the photochronocoulometric method. This technique provides a simple method for the measurement of the amount of adsorbed dyes on semiconductor surfaces. The transient photocurrent can be fit with a double-exponential decay function where the fast component is attributed to be the one-electron oxidation of the dye. The second much slower decay component can be attributed to trace reducing agents (including water) in the solution that can regenerate the reduced dye at a slow rate. By variation of the applied bias and laser intensity, the charge generated by the one-electron oxidation process and associated with the first decay stayed constant, and the rate constant displayed a linear relationship on laser power (for N3 dye) and the square root of laser power (for G7 dye). Monolayer coverages of 1.0×10^{-10} and 8.1×10^{-11} mol cm^{-2} for the N3 dye were measured for

rutile (100) and anatase (101), respectively. For the smaller molecule G7, the surface coverage is 4.1×10^{-10} mol cm^{-2} on the rutile (100) surface. The example of G7 shows that complex photochemistry can be encountered on sensitized solids; however, the photocoulometric approach provides another tool with which to study that photochemistry.

Acknowledgment. We thank Professor C. Michael Elliott for donation of purified N3 dye and the dichloro N3 dye and for helpful discussions. This work was supported by the Department of Energy Office of Basic Energy Sciences under Contract No. DE-FG03-96ER14625

References and Notes

(1) Anson, F. C.; Christie, J. H.; Osteryoung, R. A. *J. Electroanal. Chem.* **1967**, *13*, 343.
(2) Christie, J. H.; Osteryoung R. A.; Anson, F. C. *J. Electroanal. Chem.* **1967**, *13*, 236.
(3) Anson, F. C. *Acc. Chem. Res.* **1975**, *8*, 400.
(4) Turner, J. A.; Parkinson, B. A. *J. Electroanal. Chem.* **1983**, *150*, 611.
(5) Lu, Y.; Choi, D. J.; Nelson, J.; Yang, O.; Parkinson, B. A. *J. Electrochem. Soc.* **2006**, *153*, E131.
(6) (a) Fillinger, A.; Parkinson, B. A. *J. Electrochem. Soc.* **1999**, *146*, 4559. (b) Fillinger, A.; Soltz, D.; Parkinson, B. A. *J. Electrochem. Soc.* **2002**, *149*, A1146.
(7) Ushiroda, S.; Ruzycki, N.; Lu, Y.; Spitler, M. T.; Parkinson, B. A. *J. Am. Chem. Soc.* **2005**, *127*, 5158.
(8) Lu, Y.; Jaeckel, B.; Parkinson, B. A. *Langmuir* **2006**, *22*, 4472.
(9) Wang, Q.; Zakeeruddin, S. M.; Nazeeruddin, M. K.; Humphry-Baker, R.; Gratzel, M. *J. Am. Chem. Soc.* **2006**, *128*, 4446.
(10) Spitler, M. T.; Calvin, M. *J. Chem. Phys.* **1977**, *66*, 4294.
(11) Ryan, M. A.; Fitzgerald, E. C.; Spitler, M. T. *J. Phys. Chem.* **1989**, *93*, 6150.
(12) Takeda, N.; Parkinson, B. A. *J. Am. Chem. Soc.* **2003**, *125*, 5559.
(13) Bitterling, K.; Willig, F. *J. Electroanal. Chem.* **1986**, *204*, 211.
(14) Asbury, J. B.; Ellingson, R. J.; Ghosh, H. N.; Ferrere, S.; Nozik, A. J.; Lian, T. Q. *J. Phys. Chem. B* **1999**, *103*, 3110.
(15) Haque, S. A.; Palomares, E.; Cho, B. M.; Green, A. N. M.; Hirata, N.; Klug, D. R.; Durrant, J. R. *J. Am. Chem. Soc.* **2005**, *127*, 3456.
(16) Ellingson, R. J.; Asbury, J. B.; Ferrere, S.; Ghosh, H. N.; Sprague, J. R.; Lian, T.; Nozik, A. J. *J. Phys. Chem. B* **1998**, *102*, 6455.
(17) Bond, A. M.; Deacon, G. B.; Howitt, J.; MacFarlane, D. R.; Spiccia, L.; Wolfbaur, G. *J. Electrochem. Soc.* **1999**, *146*, 648.
(18) Kavan, L.; Gratzel, M.; Gilbert, S. E.; Klemenz, C.; Scheel, H. J. *J. Am. Chem. Soc.* **1996**, *118*, 6716.
(19) Wang, P.; Wenger, B.; Humphry-Baker, R.; Moser, J.-E.; Teuscher, J.; Kantlehner, W.; Mezger, J.; Stoyanov, E. V.; Zakeeruddin, S. M.; Gratzel, M., *J. Am. Chem. Soc.* **2005**, *127*, 6850.
(20) Parton, R. L.; Lenhard, J. R. *J. Org. Chem.* **1990**, *55*, 49.